



## OPEN ACCESS

## EDITED BY

Maria Iribarne,  
University of Notre Dame, United States

## REVIEWED BY

Yongchu Pan,  
Nanjing Medical University, China  
Johann Eberhart,  
The University of Texas at Austin,  
United States

## \*CORRESPONDENCE

Jacqueline T. Hecht,  
✉ jacqueline.t.hecht@uth.tmc.edu

RECEIVED 10 January 2023

ACCEPTED 21 June 2023

PUBLISHED 16 August 2023

## CITATION

Maili L, Tandon B, Yuan Q, Menezes S,  
Chiu F, Hashmi SS, Letra A, Eisenhoffer GT  
and Hecht JT (2023), Disruption of *fos*  
causes craniofacial anomalies in  
developing zebrafish.  
*Front. Cell Dev. Biol.* 11:1141893.  
doi: 10.3389/fcell.2023.1141893

## COPYRIGHT

© 2023 Maili, Tandon, Yuan, Menezes,  
Chiu, Hashmi, Letra, Eisenhoffer and  
Hecht. This is an open-access article  
distributed under the terms of the  
[Creative Commons Attribution License  
\(CC BY\)](https://creativecommons.org/licenses/by/4.0/). The use, distribution or  
reproduction in other forums is  
permitted, provided the original author(s)  
and the copyright owner(s) are credited  
and that the original publication in this  
journal is cited, in accordance with  
accepted academic practice. No use,  
distribution or reproduction is permitted  
which does not comply with these terms.

# Disruption of *fos* causes craniofacial anomalies in developing zebrafish

Lorena Maili<sup>1,2</sup>, Bhavna Tandon<sup>1</sup>, Qiuping Yuan<sup>1</sup>,  
Simone Menezes<sup>3</sup>, Frankie Chiu<sup>1</sup>, S. Shahrukh Hashmi<sup>1</sup>,  
Ariadne Letra<sup>3,4</sup>, George T. Eisenhoffer <sup>2,5</sup> and  
Jacqueline T. Hecht <sup>1,2,3\*</sup>

<sup>1</sup>Department of Pediatrics, McGovern Medical School at the University of Texas Health Science Center at Houston, Houston, TX, United States, <sup>2</sup>Genetics and Epigenetics Graduate Program, The University of Texas MD Anderson Cancer Center UTHealth Houston Graduate School of Biomedical Sciences, Houston, TX, United States, <sup>3</sup>Center for Craniofacial Research, University of Texas Health Science Center School of Dentistry at Houston, Houston, TX, United States, <sup>4</sup>Department of Diagnostic and Biomedical Sciences, University of Texas Health Science Center School of Dentistry at Houston, Houston, TX, United States, <sup>5</sup>Department of Genetics, The University of Texas MD Anderson Cancer Center, Houston, TX, United States

Craniofacial development is a complex and tightly regulated process and disruptions can lead to structural birth defects, the most common being nonsyndromic cleft lip and palate (NSCLP). Previously, we identified *FOS* as a candidate regulator of NSCLP through family-based association studies, yet its specific contributions to oral and palatal formation are poorly understood. This study investigated the role of *fos* during zebrafish craniofacial development through genetic disruption and knockdown approaches. *Fos* was expressed in the periderm, olfactory epithelium and other cell populations in the head. Genetic perturbation of *fos* produced an abnormal craniofacial phenotype with a hypoplastic oral cavity that showed significant changes in midface dimensions by quantitative facial morphometric analysis. Loss and knockdown of *fos* caused increased cell apoptosis in the head, followed by a significant reduction in cranial neural crest cells (CNCCs) populating the upper and lower jaws. These changes resulted in abnormalities of cartilage, bone and pharyngeal teeth formation. Periderm cells surrounding the oral cavity showed altered morphology and a subset of cells in the upper and lower lip showed disrupted Wnt/ $\beta$ -catenin activation, consistent with modified inductive interactions between mesenchymal and epithelial cells. Taken together, these findings demonstrate that perturbation of *fos* has detrimental effects on oral epithelial and CNCC-derived tissues suggesting that it plays a critical role in zebrafish craniofacial development and a potential role in NSCLP.

## KEYWORDS

*fos*, morphogenesis, craniofacial development, orofacial cleft, geometric morphometrics

## Introduction

Vertebrate craniofacial development relies on a complex and tightly regulated series of tissue growth and fusion, and even minor disruptions to this intricate process can lead to birth defects, the most common of which is nonsyndromic cleft lip and palate (NSCLP) (Cordero et al., 2011; Gorlin et al., 2011). The cranial neural crest cells (CNCCs) are a

multipotent population of cells that give rise to the various tissues comprising the craniofacial structures, including cartilage and bone, muscles, sensory neurons, and pigment cells (Cordero et al., 2011; Mork and Crump, 2015; Dash and Trainor, 2020). In human embryonic development, CNCCs give rise to the facial prominences during the fourth week of gestation, which over the subsequent 6–8 weeks, grow, make contact and fuse to form complete facial structures (Marazita and Mooney, 2004). Additionally, epithelial cells in the facial prominences provide important signals to CNCCs, directing their proliferation and patterning to further regulate craniofacial growth and morphogenesis (Chai and Maxson, 2006; Jiang et al., 2006). These interactions involve multiple molecular signaling pathways, including, but not limited to, wingless-type MMTV integration site family (WNT), fibroblast growth factor (FGF), bone morphogenetic protein (BMP), hedgehog (Hh) and ectodysplasin A (EDA) (Chai and Maxson, 2006; Reynolds et al., 2019).

Deficiencies in cell migration, changes in mitotic activity or apoptosis, and interruptions to epithelial-mesenchymal interactions can affect the shape and size of the facial prominences and increase the likelihood of an orofacial cleft (Jiang et al., 2006; Dixon et al., 2011; Ji et al., 2020). Quantitative studies of facial form using geometric morphometrics (GMM) have provided important information for understanding processes disrupted during craniofacial development by identifying phenotypic changes in facial prominences that contribute to orofacial clefts (Young et al., 2007).

In previous studies, we reported an association of *CRISPLD2* with NSCLP that was independently replicated in different populations (Chiquet et al., 2007; Letra et al., 2010; Shen et al., 2011; Mijiti et al., 2015; Ge et al., 2018). Further, we showed that knockdown and loss of *crispld2* in zebrafish caused severe craniofacial defects resulting from altered migration of CNCCs (Yuan et al., 2012; Swindell et al., 2015; Chiquet et al., 2018). RNA-seq analysis of *crispld2* wild type (WT) and morphant embryos revealed that *fosab* (zebrafish homologue of *FOS*) was differentially expressed. This finding, and a positive association between *FOS/rs1046117* and NSCLP, identified *FOS* as a novel candidate NSCLP gene (Chiquet et al., 2018).

*Fos* is part of the activating protein-1 (AP-1) transcription factor complex and *FOS* has roles in oncogenic processes such as tumor growth and progression, as well as biological processes like proliferation, differentiation, epithelial-to-mesenchymal transition and apoptosis (Wagner, 2002; Milde-Langosch, 2005; Durchdewald et al., 2009; Velazquez et al., 2015; Chen et al., 2017; Rodriguez-Berdini et al., 2020). *Fos* is also an activator in the lipid synthesis pathway in the endoplasmic reticulum (Wagner, 2002; Durchdewald et al., 2009; Rodriguez-Berdini et al., 2020). Mice lacking *Fos* display severe osteopetrosis, impaired gametogenesis, abnormal hematopoiesis and behavioral changes (Grigoriadis et al., 1995). Craniofacial abnormalities such as a domed skull with a shorter snout, absence of tooth eruption, as well as a reduced neocortex are also common features in *Fos* null mice (Johnson et al., 1992; Wagner, 2002; Alfaqeh et al., 2015; Velazquez et al., 2015). Importantly, reporter expression is found in orofacial tissues, including the medial edge epithelium (MEE) of the palate, the dental papilla mesenchyme, the periderm, and cells at the midline of the nasal septum of *fos-lacZ* mice (Smeyne et al., 1993a; Smeyne et al., 1993b). *Fos* protein is also detected in the

rat MEE just before the elevation of the palatal shelves, the facial epidermis, Meckel's cartilage and the mesenchymal condensations that precede bone and muscle formation (Yano et al., 1996). These studies provide strong evidence that *FOS* plays a role during craniofacial development. However, its contributions to mouth and palate formation remain to be elucidated.

Zebrafish is a commonly used animal model for craniofacial studies of embryonic development and offers many advantages that make them ideal for detailed studies, including the ability to obtain large numbers of transparent, externally developing embryos (Yelick and Schilling, 2002; Mork and Crump, 2015; Duncan et al., 2017; Raterman et al., 2020). Additionally, zebrafish craniofacial development has been well characterized and is comparable to mammalian craniofacial development (Schilling and Le Pabic, 2009; Eames et al., 2013; Mork and Crump, 2015). The ethmoid plate in zebrafish, for example, is thought to be functionally analogous to palatal development in mammals, however, there are also differences (Swartz et al., 2011; Dougherty et al., 2013; Cusack et al., 2017; Raterman et al., 2020). This study investigated the role of *fos* during craniofacial development in zebrafish using geometric morphometrics combined with tissue and cell analysis to determine its potential involvement in craniofacial morphogenesis and potential contributions to NSCLP.

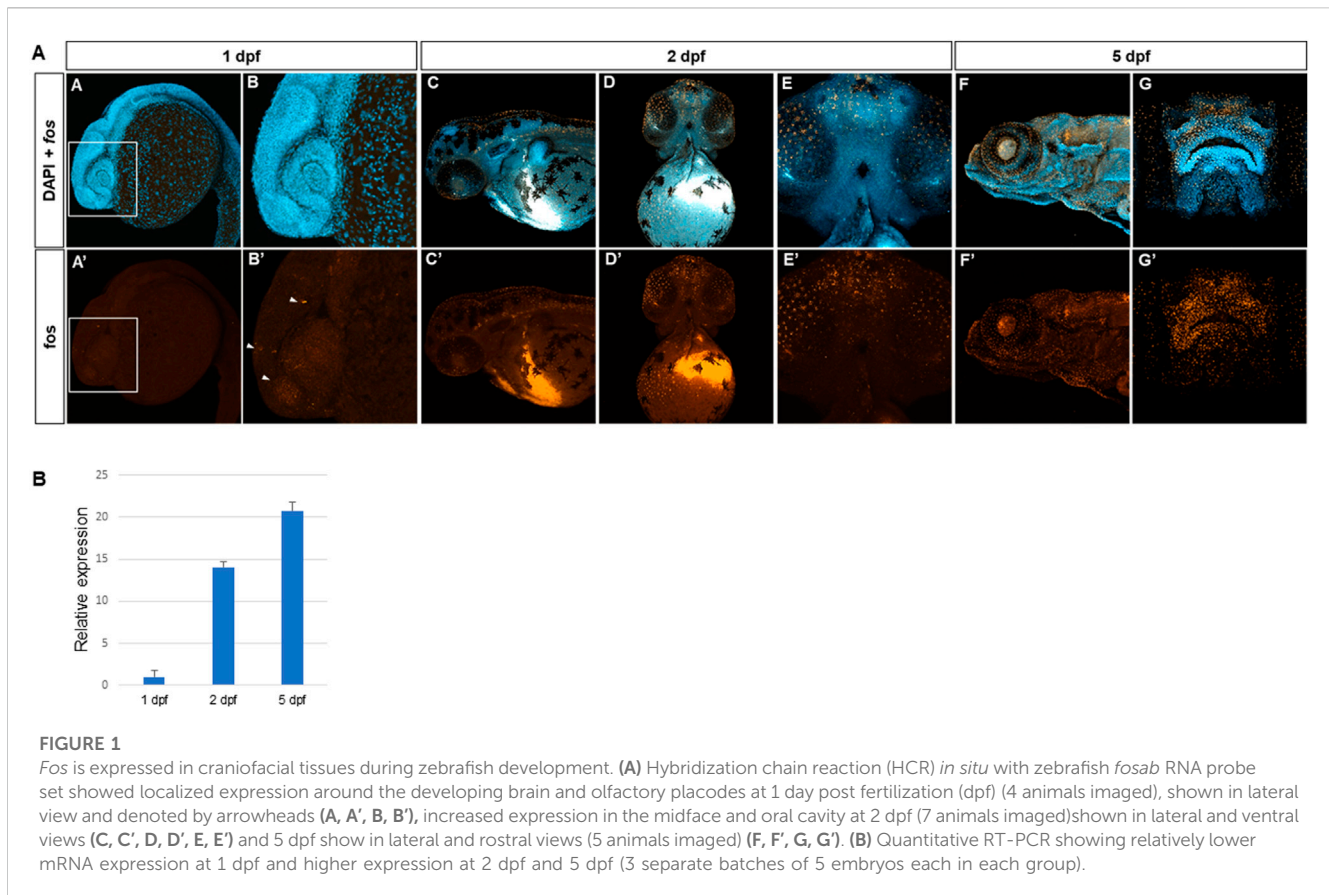
## Results

### *Fos* is expressed in midfacial and perioral regions during zebrafish development

Fluorescent *in situ* hybridization using hybridization chain reaction (HCR) (Choi et al., 2018) was used to identify *fosab* (referred to as *fos*) mRNA expression during 1–5 days post fertilization (dpf) of zebrafish development. Overall, low levels of *fos* mRNA were observed in the embryonic head at 1 dpf, however, expression was detected in a subset of tissues around the eyes (Figure 1A, A', B, B'; Supplementary Figure S1A). Increased *fos* expression was observed at 2 dpf as well as around the nares/olfactory placodes, midfacial region, eyes, oral cavity and brain (Figure 1B, 1B' 1C, 1C'). By 5 dpf, strong expression was observed in the areas surrounding the nares/olfactory pits, perioral tissues (upper and lower lips), and more diffusely in the lower jaw (Figure 1D, 1D', 1E, 1E'). Expression was also observed in the otic vesicle and lens (Figure 1D, 1D'). Examination of individual z-slices at 5 dpf showed fluorescent signal in the brain and olfactory epithelium, and the outer epithelial layer (Supplementary Figure S2). Quantitative real-time PCR of *fos* transcripts at these developmental time points were normalized to beta actin (*actb1*) and supported the *in situ* results, with lower *fos* expression observed at 1 dpf and highest at 5 dpf (Figure 1H). These findings support the expression of *fos* in craniofacial tissues throughout early development stages in zebrafish.

### *Fos* perturbation causes an abnormal phenotype in zebrafish

To define the role of *fos* in craniofacial development, zebrafish F0 mutants (referred to as *crispants*) (Burger et al.,



2016)) were generated using CRISPR/Cas9 with two single guide RNAs (sgRNAs) targeting exons 1 and 4 of the *fos* gene. Genotyping revealed efficient mutagenesis with 89% of embryos showing a deletion of approximately 1,500 base pairs (bp) of the *fos* coding region (Figure 2A). F0 embryos (84%) displayed an abnormal phenotype at 5 dpf, with smaller head and eyes, cardiac edema, abnormal yolk extension, missing swim bladder and curved body axis compared to uninjected control embryos (UIC) and tyrosinase sgRNA-injected F0 embryos (0%) (Figures 2B,C; Supplementary Figure S4). Abnormal mouth shape, displaced and merged neuromasts (arrowheads), and anomalies in lower jaw tissues were observed (Figures 2D,E). *In situ* hybridization showed reduced *fos* mRNA expression in the head at all developmental time points examined (Supplementary Figure S1). A small number of embryos (16%) appeared normal, likely reflecting mosaicism resulting from F0 CRISPR mutagenesis. Stable *fos* mutants (F2 generation) with the same deletion as F0 crispants had significantly reduced *fos* mRNA levels and a normal phenotype. Genetic compensation studies of closely related genes showed that *fosb* was significantly upregulated in the mutants at both 2 and 3 dpf ( $p = 0.03$  and  $0.006$  respectively) (Supplementary Figure S3). Moreover, providing additional evidence for *fos* excision in these animals, injection of the *fos* sgRNAs into the stable F2 mutants did not cause an abnormal craniofacial phenotype (Supplementary Figure S4A).

To further evaluate the consequences of reduced *fos* on craniofacial development, a translation-blocking morpholino (MO) against *fos* was used. *Fos* morphant embryos displayed similar abnormalities to crispants at 5 dpf (Figures 2F,H), while mismatch (MM) control injected embryos were similar to the UICs (Figures 2G, I). Co-injection with a morpholino directed to p53 did not improve the phenotype, supporting that the abnormal morphant phenotype was independent of non-specific cell death (Boer et al., 2016) (Supplementary Figure S4B). Additionally, *fos* MO was injected in stable *fos* F3 mutants and did not lead to an abnormal phenotype, supporting the specificity of the *fos* MO. To further test the specificity of *fos* knockdown, human FOS (Hu-FOS) mRNA, which is not targeted by zebrafish *fos* MO, was co-injected and rescued the morphant abnormalities including the size of the head and eyes, as well as oral cavity shape (Figures 2J, K). While 82% of *fos* morphants had an abnormal mouth and face, only 45% had an abnormal phenotype after human FOS mRNA co-injection (Supplementary Figure S5A). Interestingly, overexpression of human-FOS RNA, as well as zebrafish *fos* mRNA, caused severe facial abnormalities, including an extended lower jaw and cyclopia in more than 50% of surviving injected embryos (Figures 2L, M). Pharmacological perturbation of AP-1 transcription factor complex activity mediated by *fos* using SR 11302 resulted in craniofacial abnormalities, similar to those observed in *fos* crispant and morphant embryos, including a narrow face, smaller mouth,

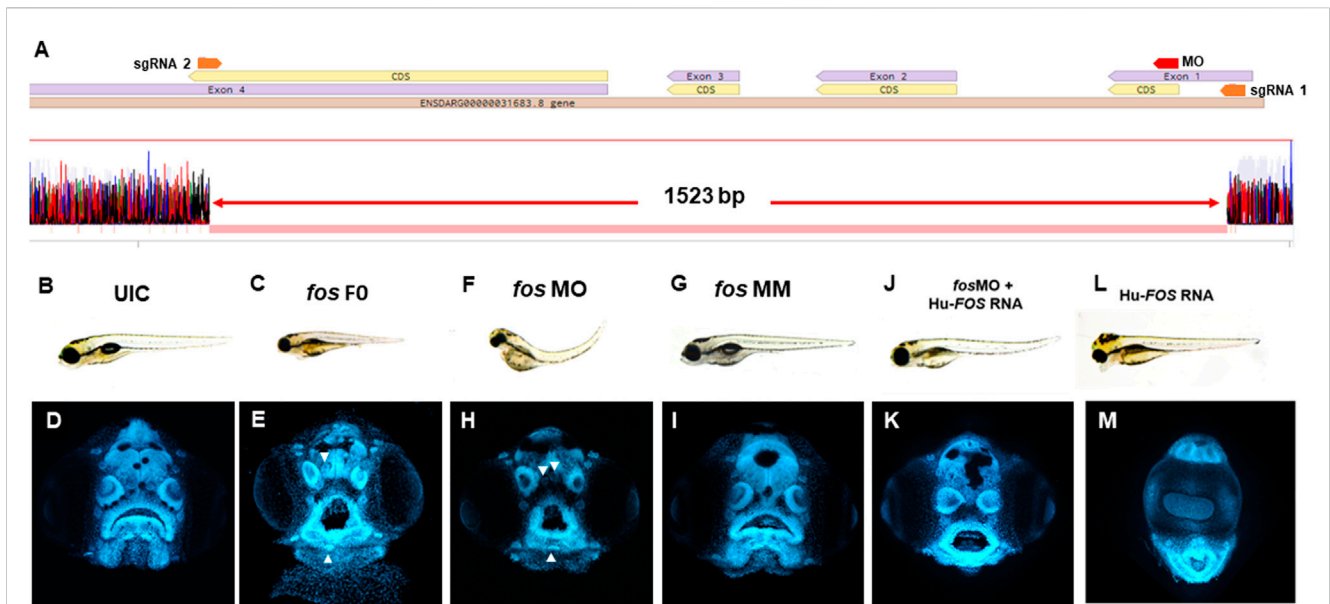


**FIGURE 2**

*Fos* mutants and morphants have distinctive keyhole-shaped mouth and abnormal craniofacies. (A) Schematic of CRISPR guides targeting exons 1 and 4 of the *fosab* gene and resulting in an almost complete deletion of the coding region with a 1.523 kb deletion confirmed by DNA sequencing. (B–L) Representative brightfield images of 5dpf zebrafish showing normal phenotype (B) and abnormalities in *fos* F0 mutants (15/24 embryos, 63%) and morphants (102/132 embryos, 77%) (C and F) compared to UIC and MM controls (110/122 embryos, normal phenotype, 90%) (B, G). (D–M) Confocal images of rostrally mounted DAPI-stained samples showed a distinctively abnormal facial and mouth shape in both *fos* mutant (103 embryos) (H) and morphant (138 embryos) (I) embryos compared to UIC (93 embryos) (D) and MM (47 embryos) controls (I). Arrowheads indicate merged or displaced neuromasts. Co-injection of human *FOS* mRNA rescued the morphant phenotype (J and K) while overexpression alone caused other abnormalities including cyclopia and an elongated lower jaw (L, M). UIC, uninjected control; F0, crispant; MO, morpholino; MM, mismatch; Hu-FOS, human *FOS* mRNA.

**TABLE 1 Results of morphometric analysis *Fos* crispants (F0 mutants), morphants and MO + mRNA co-injected (rescue) embryos were compared using morphometric analysis of the facial region.**

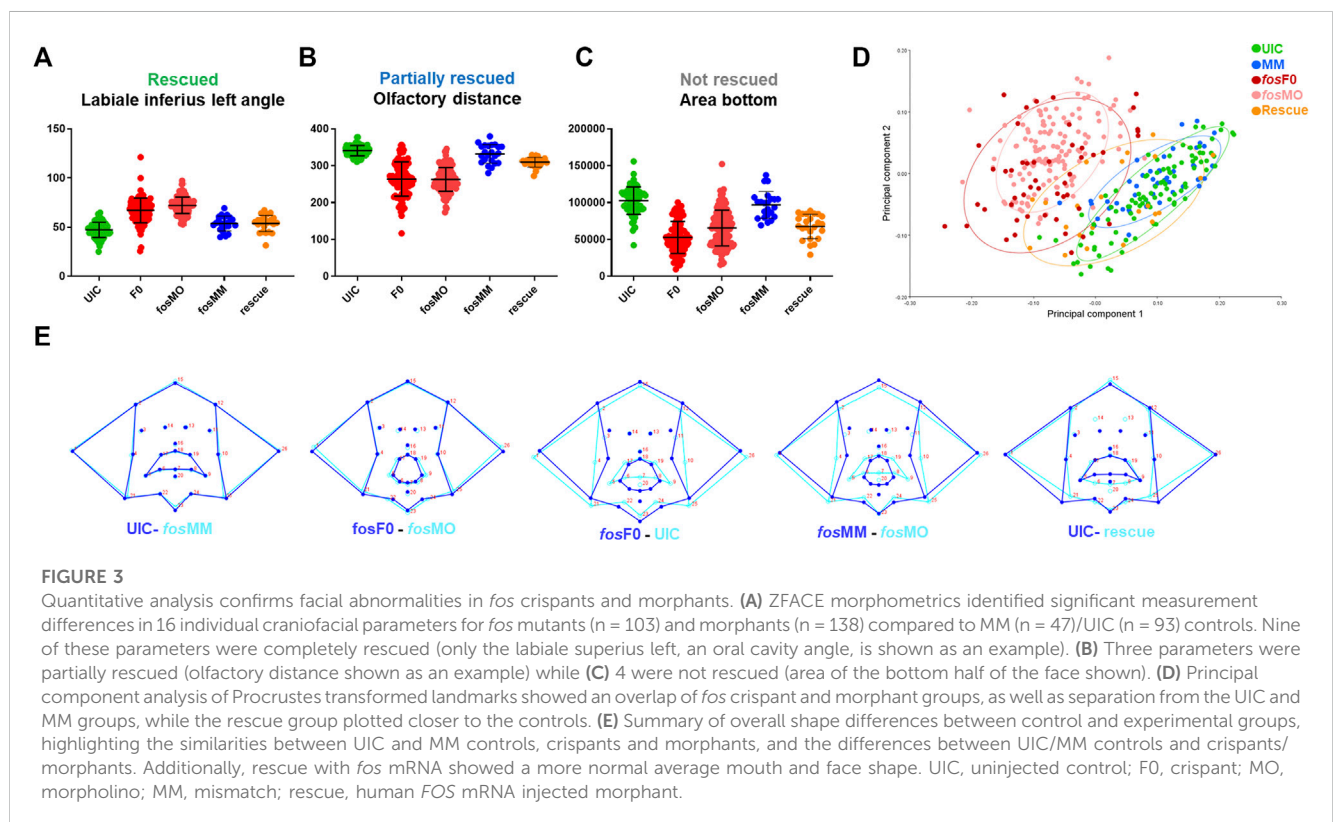
zFACE feature	ANOVA	fos F0 mutants		fos morphants			rescue		Summary
		UIC vs. F0	UIC vs. fosMO	UIC vs. fosMM	fosMM vs. fosMO	fosMOvs.F0	UIC vs. rescue	fosMO vs. rescue	
Olfactory to Mouth 2	<0.0001	<0.0001	<0.0001	n.s.	0.0003	n.s.	n.s.	<0.0001	rescued
Olfactory to Mouth 3	<0.0001	<0.0001	<0.0001	n.s.	0.0002	n.s.	n.s.	<0.0001	rescued
Mouth Height	<0.0001	<0.0001	<0.0001	n.s.	<0.0001	n.s.	n.s.	<0.0001	rescued
Labiale Inferius Angle	<0.0001	<0.0001	<0.0001	n.s.	<0.0001	0.008	n.s.	<0.0001	rescued
Crista Phillri LeftAngle	<0.0001	<0.0001	<0.0001	n.s.	<0.0001	0.005	0.002	<0.0001	rescued
Crista Phillri Right Angle	<0.0001	<0.0001	<0.0001	n.s.	<0.0001	n.s.	0.005	<0.0001	rescued
Labiale Superius Mid Angle	<0.0001	<0.0001	<0.0001	n.s.	<0.0001	0.003	n.s.	<0.0001	rescued
Labiale Inferius LeftAngle	<0.0001	<0.0001	<0.0001	n.s.	<0.0001	n.s.	n.s.	<0.0001	rescued
Labiale Inferius Right Angle	<0.0001	<0.0001	<0.0001	n.s.	<0.0001	n.s.	n.s.	<0.0001	rescued
Olfactory Distance	<0.0001	<0.0001	<0.0001	n.s.	<0.0001	n.s.	<0.0001	<0.0001	partial rescue

(Continued on following page)

**TABLE 1 (Continued)** Results of morphometric analysis *Fos* crispants (F0 mutants), morphants and MO + mRNA co-injected (rescue) embryos were compared using morphometric analysis of the facial region.

zFACE feature	ANOVA	fos F0 mutants		fos morphants			rescue		Summary
		UIC vs. F0	UIC vs. fosMO	UIC vs. fosMM	fosMM vs. fosMO	fosMOvs.F0	UIC vs. rescue	fosMO vs. rescue	
Neuromast Width	<0.0001	<0.0001	<0.0001	n.s.	<0.0001	0.002	<0.0001	0.002	partial rescue
Mouth Perimeter	<0.0001	<0.0001	<0.0001	n.s.	<0.0001	n.s.	<0.0001	<0.0001	partial rescue
Chin Width	<0.0001	<0.0001	<0.0001	n.s.	<0.0001	n.s.	0.003	n.s.	not rescued
Neuromast Angle 2	<0.0001	<0.0001	<0.0001	n.s.	<0.0001	n.s.	0.002	n.s.	not rescued
Area Bottom	<0.0001	<0.0001	<0.0001	n.s.	<0.0001	n.s.	<0.0001	n.s.	not rescued
Area Combined	<0.0001	<0.0001	<0.0001	n.s.	<0.0001	0.005	0.0002	n.s.	not rescued

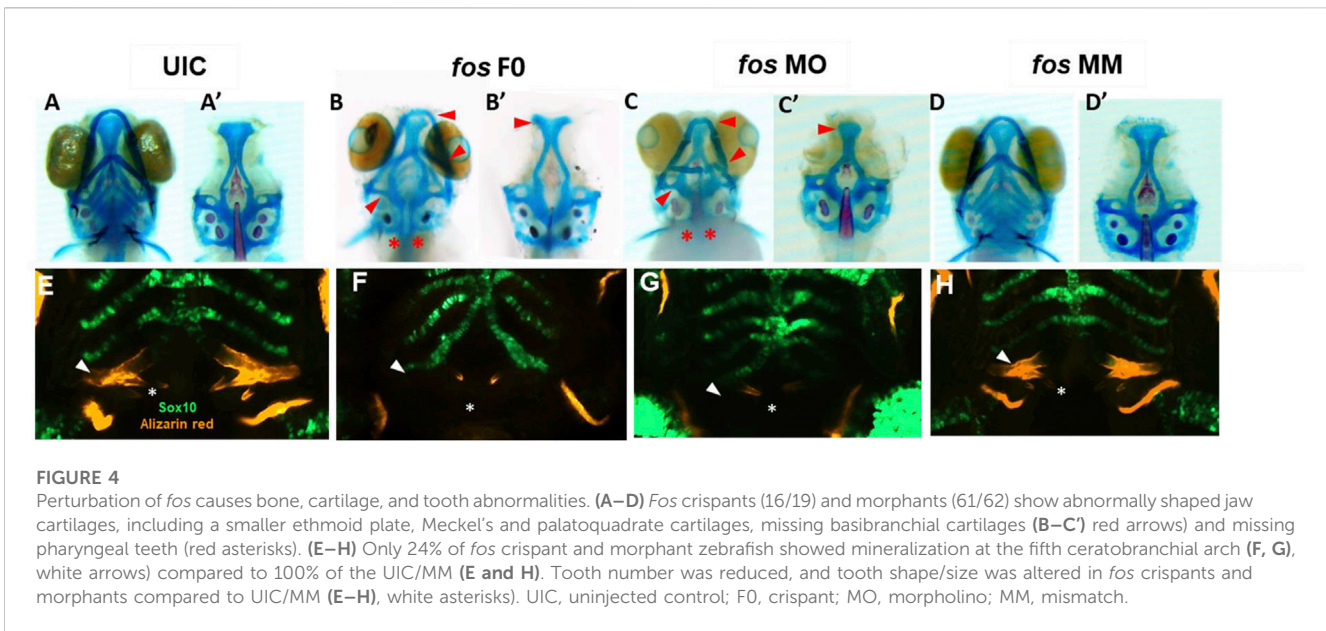
ANOVA, analysis of variance; n.s., not significant.



and altered olfactory pits (Supplementary Figure S6). As expected, this resulting phenotype was more severe because of the wider range of disruption by the AP-1 inhibitor, which targets the AP-1 dimer complex composed of different members of the *fos* and *jun* protein families (*fos*, *fosb*, *fra-1*, *fra-2*, *jun*, *junB*, *junD*) (Wagner, 2002). AP-1 inhibitor treatment led to a more severe mouth phenotype in stable F3 *fos* mutants compared to wild type and DMSO treated groups, suggesting that while the stable mutants have a normal phenotype, they are more sensitive to AP-1 perturbations (Supplementary Figure S6). Taken together, these results suggest a key role for *fos* in regulating craniofacial development in zebrafish embryos.

## Geometric morphometric analysis identifies orofacial features altered by *fos*

To identify the orofacial features altered by genetic perturbation of *fos* at 5 dpf, we used zFACE, a geometric morphometric tool for quantitative deep phenotyping of the craniofacial region in zebrafish embryos (Maili et al., 2023). This tool uses 26 anatomical landmarks, comparable to those used in human geometric morphometric (GMM) studies (Weinberg et al., 2008), to calculate 39 facial measurements, including linear distances, areas and angles (Maili et al., 2023). As shown in Table 1, significant alterations were observed for



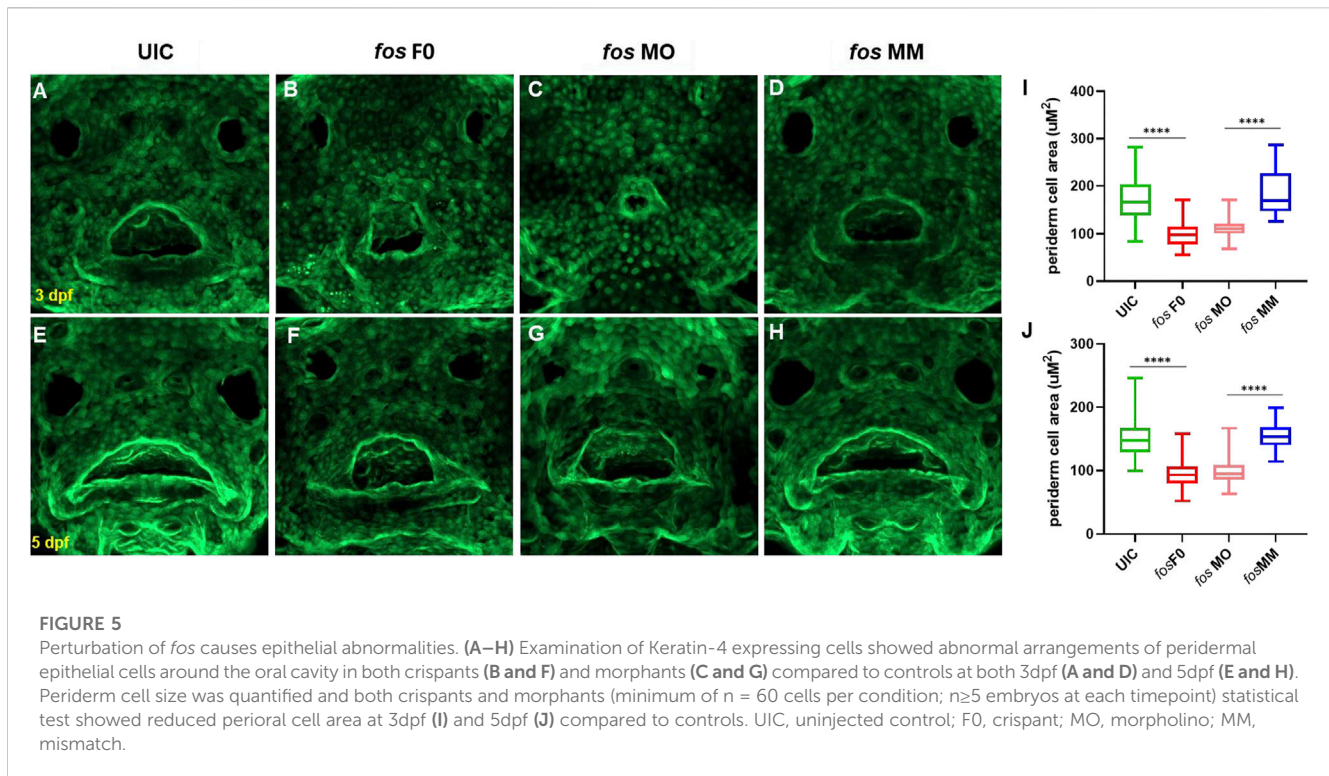
16 facial features in both *fos* crispants and morphants compared to UIC and MM controls (ANOVA with *post hoc* Tukey's test,  $p < 0.0001$ ). These included differences in oral cavity dimensions and angles, olfactory placode positioning, as well as area measurements in the lower half of the face. Similar phenotypic results were observed at 6 dpf, indicating that the facial anomalies did not improve with time and were not the result of a delay in development (Supplementary Figure S7; Supplementary Table S1). Nine of the 16 altered dimensions (2 olfactory to mouth angles, mouth height, and 6 oral cavity angles) were fully rescued by Hu-FOS mRNA injection (Table 1; Figure 3A). Olfactory distance, neuromast width and mouth perimeter were partially rescued; they were different compared to the controls and to the morphants, representing an intermediate phenotype (Table 1; Figure 3B). Four facial features, chin width, a neuromast angle, area bottom and area combined, were not rescued (Table 1; Figure 3C). Morphometric analysis could not be performed in the overexpression group due to the severity of the phenotype and many anatomical landmarks missing.

Unbiased multivariate analysis using principal component analysis (PCA) was next performed after Procrustes transformation to determine overall shape changes after *fos* disruption. The first two components (PC1, PC2) were responsible for 63% of the variance in the dataset. Landmarks in the lower part of the oral cavity and midface had the largest vectors of change across PC1, while landmarks outlining the lower jaw, location of the pupils and upper lip had the largest vectors of change across PC2 (Supplementary Figure S8). A component plot for PC1 and PC2 showed overlap of *fos* crispant and MO groups, as well as separation of the crispant and MO groups from the UIC and MM controls (Figure 3D). A small subset ( $n = 5$ , 10%) of crispants clustered close to the UIC and MM control groups, likely due to mosaicism. The rescue group mapped closer to the control groups, with some individuals in the intermediate area of the plot, likely reflecting the partial rescue observed in the previous analysis (Figure 3D).

Shape analysis was also performed using discriminant function analysis (DFA) to determine face shape differences between experimental and control groups (Klingenberg, 2011). As expected, face shape in UIC and MM controls was similar (Procrustes distance = 0.03,  $p = 0.06$ ). Although a significant difference was found between *fos* crispants and morphants, comparison of wireframe representations revealed only minor alterations in face shape (Procrustes distance = 0.06,  $p < 0.001$ ) (Figure 3E). Comparisons between both crispants to UICs (Procrustes distance = 0.18,  $p < 0.001$ ) and morphants to MM controls (Procrustes distance = 0.17,  $p < 0.001$ ) showed significant shape differences involving the oral cavity, midface and lower jaw in both comparisons (Figure 3E). DFA also highlighted the improvement in the rescue group when compared to UICs, specifically in the upper lip and upper face regions, however the lower lip and jaw landmarks remained abnormal (Figure 3E). Together, these quantitative analyses demonstrated that perturbation of *fos* affected oral cavity and midface dimensions and overall facial shape.

## Fos perturbation alters craniofacial structures

Given that the shape of the underlying skeletal tissues is a major contributing factor to facial shape, the bone and cartilage based structures that comprise craniofacial tissues were examined (Murillo-Rincon and Kaucka, 2020). Skeletal staining showed reduced and abnormally shaped jaw cartilages, including smaller ethmoid plate, trabeculae and parachordal cartilages, reduced Meckel's and palatoquadrate cartilages and missing basibranchial cartilages in both *fos* crispants and morphants (Figures 4B, B', C, C') compared to UIC and *fos* MM controls (Figures 4A, A', D, D'). The parasphenoid bone, branchiostegal rays and fifth ceratobranchial arches (CB5) showed impaired ossification and smaller or missing pharyngeal teeth (Figures 4 B-C, asterisks). Fused otoliths and



asymmetric neurocranial structures were also observed (Figure 4C'). Morphants generally displayed a more severe disruption of the craniofacial skeleton. These cranioskeletal abnormalities were dose-dependent, ranging from mild (0.5ng/uL MO injection) to very severe (2ng/uL MO injection) (Supplementary Figure S9).

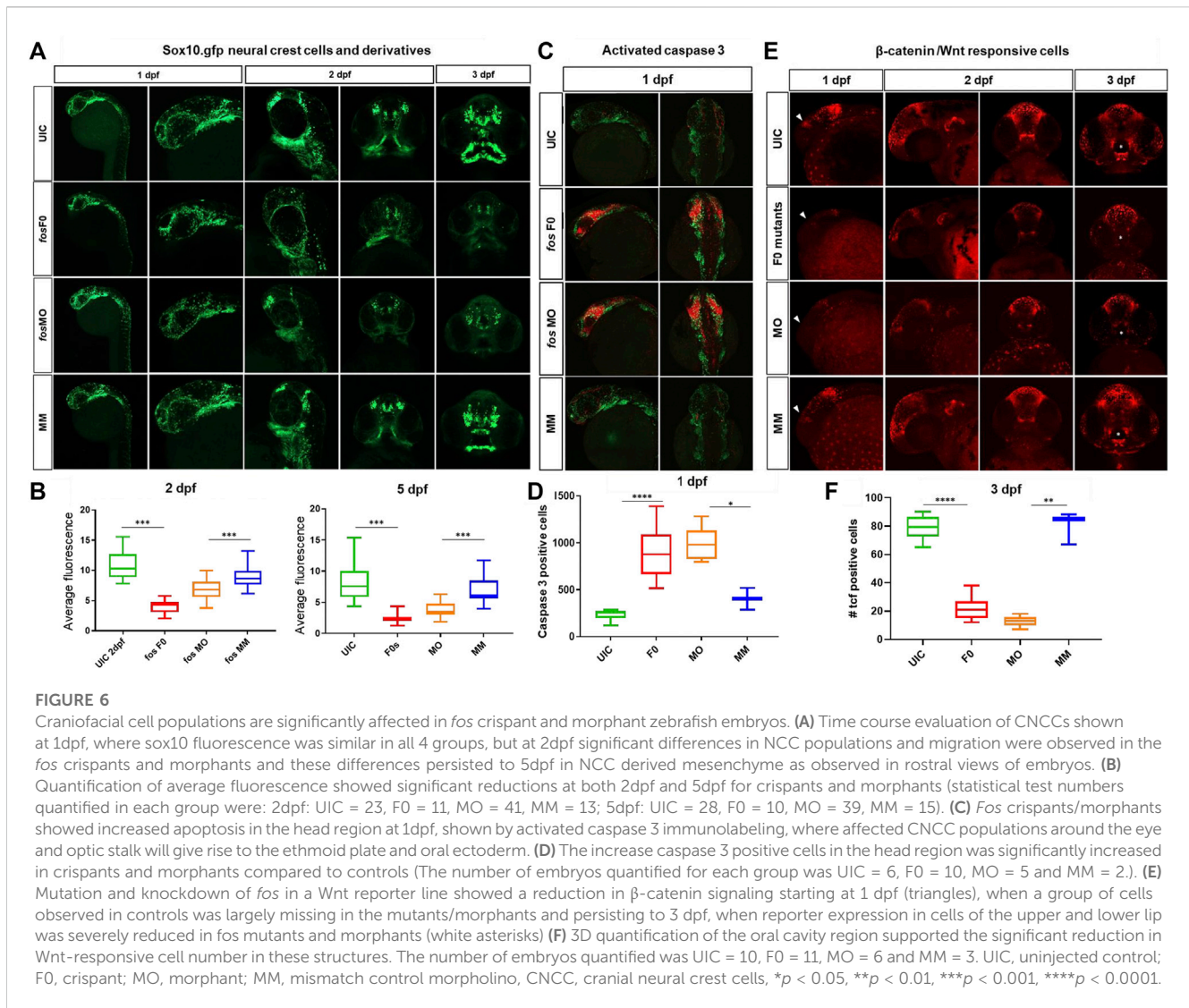
Abnormal pharyngeal/branchial arch formation was suggested based on the multiple bone and cartilage anomalies. *Fos* knockdown in the Tg (-4.9sox10:GFP) zebrafish line was used to visualize the developing pharyngeal arches (PAs) (Carney et al., 2006). At 5dpf, PAs 1 and 2 were abnormal, with crispants/morphants showing cellular disorganization, vertical and horizontal constrictions and arch asymmetry (Supplementary Figure S10). Approximately 20% of crispant, and 37% of morphant larvae showed merged PA1 and PA2; while all crispants/morphants had abnormally-shaped but intact PAs 3–7 (Figure 4G–H; Supplementary Figure S10). Additionally, mineralization of the fifth ceratobranchial (CB5/PA 7), visualized by alizarin red staining, was observed in 100% of the UIC and MM embryos, compared to only 19% of *fos* crispants and 24% of morphants (Figures 4E–H arrow; Supplementary Figure S11; Supplementary Table S2). Decreased mineralization persisted during subsequent developmental stages, with only 68% of morphants showing evidence of mineralization by 8dpf (Supplementary Figure S11D). Smaller cleithrums and opercles were also observed, indicating abnormal ossification in craniofacial dermal bones (Figure 4E–H).

Development of zebrafish pharyngeal dentition was also examined in *fos* crispants and morphants. At 5dpf, 3 bilateral rows of pharyngeal teeth (4V1, 3V1 and 5V1), were observed in both UIC and MM controls, with 4V1 ankylosed/attached to the perichondral bone of CB5, as expected (Figures 4E,H; Supplementary Figure S11C). In comparison, crispant and

morphant larvae had only 1 tooth (4V1) on each side of the arch, which was smaller and of abnormal morphology compared to the controls. In mild phenotypic crispants/morphants, 4V1 had attached/deposited bone around the non-mineralized CB5 cartilage, while in crispants/morphants showing severe phenotypes only 4V1 buds were visible (Figures 4F,G; Supplementary Figure S11C). Defects in tooth attachment, morphogenesis, and in CB5 mineralization persisted to 8dpf (Supplementary Figure S11D; Supplementary Table S2). These abnormalities in bone, cartilage, pharyngeal arch and tooth formation in both *fos* crispants and morphants are consistent with perturbation of a common developmental program.

## Epithelial and neural crest cell alterations result from *fos* disruption

Cell populations important for craniofacial development in *fos* crispants and morphants were next examined to understand the abnormal phenotype resulting from *fos* perturbation. Since expression of *fos* mRNA was detected in the outer epithelial layer, epithelial cell number and morphology were analyzed using a keratin-4 transgenic reporter line Tg(*krt4:gfp*) (Gong et al., 2002). *Fos* crispants and morphants showed abnormal cellular arrangement, particularly around the oral cavity and nares/olfactory pits compared to UIC and MM controls at 3 and 5 dpf (Figures 5A–D). Visualization of the borders and cell-cell junctions of epithelial cells also further showed the smaller oral cavities and olfactory pits in crispants/morphants (Figures 5E–H). In addition to altered arrangement of epithelial cells around the oral cavity and lower jaw, cells in the perioral region of both crispants and



morphants had a smaller area compared to controls at both 3 dpf ( $p < 0.0001$ , Student's *t*-test) and 5 dpf ( $p < 0.0001$ ) (Figure 5 I, J; see Supplementary Figure S12 for a description of facial region analyses). These results suggested a role for *fos* in regulating epithelial cell size and arrangement around the oral cavity.

The transgenic line *Tg(-4.9sox10:EGFP)* (Carney et al., 2006) that labels pre-migratory and migrating CNCCs was used to examine these cells because of their large contributions to craniofacial bone and cartilage. Early in development (1 dpf, Figure 6A) CNCC numbers and migration were unaffected in the crispants and morphants when compared to controls ( $p = 0.27$ ). However, by 2 dpf, significant differences were observed in the number and migration pattern of CNCCs in *fos* crispants and morphants ( $p < 0.0001$ ) (Figures 6A,B). At 3 dpf, crispants and morphants continued to show reduced CNCC derivatives compared to both UICs and MMs and these differences were more pronounced at 5 dpf, with significant decrease of GFP fluorescence in crispants/morphants compared to UIC controls ( $p < 0.0001$  for both, Figures 6A,B). Immunostaining for activated caspase-3 showed a dramatic increase in the number of positively stained cells around the eyes and

in the midline in both crispants and morphants suggesting high, localized cell death between 1 dpf and 2 dpf (Figure 6C). While MOs are known to cause an increase in cell death (Boer et al., 2016), very similar results were also observed in the F0 crispant larvae, suggesting this precocious death is promoted by a lack of *fos*. Together, these results demonstrated that absence/knockdown of *fos* compromised the survival of critical subpopulations of CNCCs and contributed to the phenotypic anomalies observed later in development.

Interactions between the mesenchyme and epithelial cells are known to induce Wnt signaling centers that control cell fates and behaviors in the surrounding tissues (Jussila and Thesleff, 2012). Based on the changes observed in CNCC derivatives and epithelial cells, a reporter zebrafish line that serves as a biosensor for Wnt signaling (*Tg(7xTCF-Xla.Siam:GFP)*) was evaluated for changes in  $\beta$ -catenin mediated Wnt activity (Moro et al., 2012). A general reduction in WNT-responsive cells, in both *fos* crispants and morphants, was identified in the head starting at 1 dpf and 2 dpf ( $p < 0.01$ , Figure 6; Supplementary Figure S13). At 3 dpf, we observed a group of WNT responsive cells that were restricted to the upper

and lower lip. Intriguingly, a dramatic reduction of these Wnt responsive cells was observed in both *fos* crispants and morphants (Figure 6, asterisks). Quantification of these cells in 3D analysis using Imaris supported the significantly reduced number of reporter positive cells in the oral cavity region ( $p = 4.08E-12$  and  $p = 0.007$ , crispants compared to UIC and morphants compared to MM controls, respectively). By 5dpf,  $\beta$ -catenin active cells had recovered around the oral cavity in crispants/morphants, however the organization of the cells followed the abnormal mouth shape. Together, these results suggested that Wnt responsive cells were reduced at early developmental time points and severely disrupted around the mouth at 3dpf, implicating that absence or reduction of *fos* impacted the ability of these cells to properly pattern the oral cavity.

## Discussion

*Fos* plays a role in embryonic and craniofacial development (Wagner, 2002; Durchdewald et al., 2009; Alfaqeeh et al., 2015; Velazquez et al., 2015) and was previously identified in a network of differentially expressed genes in a zebrafish model of orofacial clefts and confirmed in a human family-based association study (Chiquet et al., 2018). In this study, we sought to characterize the role of Fos in orofacial morphogenesis and oral cavity formation. Using both *fos* crispant and morphant embryos, we showed that absence or reduction of *fos* in developing zebrafish led to an abnormal craniofacial morphology with a distinctive abnormal ovoid oral cavity shape, suggesting a key role in orofacial morphogenesis. Deep phenotyping using geometric morphometric analyses showed that midface dimensions and oral cavity shape were the facial features most affected by *fos* perturbation. Further, perioral epithelial cells had altered morphologies and cranial neural crest cells (CNCCs) were reduced in number. These changes corresponded to a reduction in Wnt-responsive cells around the oral cavity, suggesting that *fos* plays an important regulatory role in guiding the interactions between the epithelial and mesenchymal cell populations that induce WNT signaling during oral cavity development. Together, our findings provide a better understanding of the contributions of *fos* in vertebrate craniofacial development and suggest that variation in *FOS* expression can alter facial dimensions during development and potentially play an etiologic role in orofacial clefting.

Cell migration and movements during craniofacial development facilitate interactions between different cell and tissue types, and their environment (Murillo-Rincon and Kaucka, 2020). These interactions are critical to create spatially defined sources of morphogenetic signals (e.g., WNTs, FGFs, BMP, Hedgehog), commonly referred to as signaling centers or organizers (Perrimon et al., 2012; Martinez Arias and Steventon, 2018; Murillo-Rincon and Kaucka, 2020). Both the initiation of the signaling centers in the developing head and the expression levels of inductive signals can be modified by several mechanisms, such as 1) changes in gene expression that perturb survival or migration of specific cell types and 2) the timing of the cell/tissue interactions (Perrimon et al., 2012).

Although CNCC death can be associated with morpholino oligonucleotide use (Boer et al., 2016), the marked upregulation

of apoptosis of CNCC in the head and around the eyes was also identified in the crispants, but not in mismatch morpholino injected embryos. These results suggest that the observed apoptosis is not solely due to morpholino-related toxicity. Importantly, areas in which increased caspase-3 was detected at 1dpf also showed specific regional *fos* mRNA expression. The CNCC in these regions have been shown to migrate rostrally and caudally to reach the oral ectoderm and ethmoid plate (Eberhart et al., 2008) and the observed aberrant apoptosis likely led to the regional reduction of CNCCs, resulting in abnormal arches and anomalous jaw skeletal elements. Indeed, *fos* knockdown has been shown to cause increased apoptosis in osteosarcoma cells (Wang et al., 2017), supporting the relationship between reduced levels of *fos* and increased apoptosis observed in our crispant and morphant zebrafish models. In *C. elegans*, *fos* is also a cell autonomous regulator of cell invasion, a process critical for many cell types and also NCCs, as they need to invade through extracellular matrix, mesoderm and migrating endothelial cells to reach their destination, making their motility and invasive ability crucial (Sherwood et al., 2005; McLennan et al., 2020). Overall, perturbation of zebrafish *fos* expression affected the survival and migration of a specific subset of NCCs that populate the oral ectoderm and ethmoid plate, suggesting that one of the mechanisms responsible for the abnormal orofacial phenotype is the early disruption of NCCs.

Epithelial-mesenchymal interactions play a crucial role during the development of several organs and tissues and are mediated by cell-cell contact, or the diffusion of soluble factors such as Wnts (Ribatti and Sautoiemma, 2014). During tooth development, regional signals from the ectoderm induce molecular changes in the cranial neural crest-derived ectomesenchyme (Jussila and Thesleff, 2012). The activation of  $\beta$ -catenin signaling is required in the oral epithelium for the induction of placodes and formation of enamel knots; this signaling is also necessary in the odontogenic mesenchyme beyond the bud stage (Chen et al., 2009; Jussila and Thesleff, 2012). Both *fos* crispants and morphants showed a dramatic reduction of Wnt-responsive cells around the oral cavity at 3dpf, whereas the brain was less affected, indicating that Wnt signaling was perturbed in this region. Consistent with disrupted inductive signaling, *fos* crispants/morphants showed abnormal tooth development, with marked delays in tooth formation and anomalies in morphology and number of teeth. Even though the process of tooth eruption in mice is different from pharyngeal tooth attachment to CB5 in zebrafish, these results are consistent with observations of smaller teeth in *Fos* null mice that fail to erupt and form roots (Van der Heyden and Huisseune, 2000; Alfaqeeh et al., 2015).

The periderm serves important functions in craniofacial structures that fuse during development, such as the oral cavity and the palate (Hammond et al., 2019). In mammalian models, abnormal periderm development leads to epithelial adhesions and orofacial clefts, while failure of periderm removal from fusing palatal shelves can contribute to cleft palate (Richardson et al., 2014; Hammond et al., 2019). Periderm anomalies were observed starting at 3dpf in the perioral region, suggesting that loss of *fos* could also be contributing to peridermal abnormalities linked to abnormal orofacial development. Future experiments will identify how *fos* regulates the molecular mechanisms in periderm cells.

Interestingly, our results showed that at 3 dpf, CNCC derivatives were greatly reduced in the upper and lower jaws, at the same time that oral periderm cells showed altered morphologies and arrangement, indicating that perturbation of *fos* interrupted both epithelial and mesenchymal cell populations around the developing oral cavity. This specific effect on cells around the oral cavity corresponds with the mouth and midface shape anomalies detected at 5 dpf, suggesting a disruption to critical inductive signals that regulate orofacial morphology. This could result from either missing  $\beta$ -catenin active cells or inability of these cells to activate  $\beta$ -catenin signaling and warrants further studies. These findings suggest that *fos* plays an important inductive role in regulating interactions between epithelial and mesenchymal cell populations and its absence affects both cells around the oral cavity and midface and mineralized tissue like bones and teeth.

Additionally, Wnt/ $\beta$ -catenin signaling delineates areas of rapid growth in the facial prominences in murine models, and both genetic and pharmacologic perturbation of this signaling pathway results in altered craniofacial dimensions during embryonic development (Brugmann et al., 2007; He and Chen, 2012). The use of geometric morphometrics allowed identification of regional alterations to dimensions such as mouth height, olfactory to mouth angles and olfactory distance, and identified significant shape changes to the mouth and midface, strongly supporting the role of *fos* in morphogenesis of these structures (Maili et al., 2023). Together with the reduced number of Wnt responsive cells in the perioral region, these findings suggest insufficient growth in these tissues when *fos* is absent or reduced. Interestingly, a correlation between the dimensions of the maxillae and nasal pits and susceptibility for developing cleft lip and palate has been reported in mice (Young et al., 2007; Parsons et al., 2008; Green et al., 2015). Additionally, human morphometric studies have shown that there are facial differences in the upper lip, philtrum and nasolabial angles in individuals predisposed to orofacial clefts as well as their unaffected relatives (Fraser and Pashayan, 1970; Weinberg et al., 2006a; Weinberg et al., 2006b; Weinberg et al., 2009; El Sergani et al., 2020). Together with the findings that variation in *FOS* is associated with NSCLP, these results suggest that altered *fos* expression affects the growth and shape of the oral cavity and midface regions and potentially plays an etiologic role in the development of an orofacial cleft.

Crisprants, morphants and pharmacologic inhibition of the AP-1 transcription factor complex produced similar orofacial anomalies, supporting our findings. In the majority of surviving larvae, *fos* mRNA overexpression also caused a cyclopia craniofacial phenotype suggesting possible connections between dysregulated *fos* expression and ciliopathies and/or other developmental signaling pathways such as Nodal or Hedgehog. Stable *fos* mutants (F1, F2, F3 generations) had no phenotype even though they had 1.5 kb deletions and absent *fos* mRNA expression and thus were not useful for these studies. Similar results from multiple studies suggest that this is likely related to genetic compensation unique to Crispr/Cas9 mutagenesis methods (Rossi et al., 2015; Buglo et al., 2020). Increased expression of *fosl1a*, *fosb* and *fosl2* was observed in the *fosab* mutants (Supplementary Figure S3). Additionally, injection of the guide RNAs in *fosab* mutant embryos did not produce a phenotype, however, these stable mutants were more sensitive to

pharmacological AP-1 disruption (Supplementary Figure S4, S6). These data support the idea that compensatory mechanisms by similar gene family members may be responsible for buffering the phenotype.

In conclusion, this study demonstrates that *fos* is critical for zebrafish craniofacial development and *fos* perturbation affects multiple craniofacial tissues resulting in abnormal orofacial structures. Loss of *fos* has a profound effect on facial progenitor cells, suggesting that it is important for epithelial and mesenchymal cell populations and regulates interactions between them that are crucial for proper oral cavity morphogenesis. Although cleft lip was not seen in our zebrafish embryos, severe orofacial anomalies were observed. This result may be related to species-specific differences in mouth development (Soukup et al., 2013). Based on the current work as well as results suggesting a role for *FOS* in NSCLP (Chiquet et al., 2018), future investigations in zebrafish and humans should target identification of other genes and pathways by which *fos* regulates craniofacial development.

## Materials and methods

### Zebrafish care and husbandry

Zebrafish (*Danio rerio*) were housed and maintained at 28°C as described previously (Westerfield, 1993). All work involving the use of animals was performed with approval of the UTHealth Animal Welfare Committee (AWC-20-0052).

### Morpholino, mRNA and CRISPR/Cas9 injections

Zebrafish *fos* antisense morpholinos (Fos MO: GCGTTAAGGCTG GTAAACATCATCC) targeting the ATG start site in exon 1 and a mismatched control (Fos MM: GaGTTAAcGCTcGTAAaATCATaC, mismatch in small caps) were designed by GeneTools (Philomath, OR). Morpholinos were suspended in MilliQ water to a stock concentration of 16.67 mg/mL or 2 mM. Injections of morpholinos were diluted to 0.5 ng/ $\mu$ L to 3 ng/ $\mu$ L in Danieau buffer. A plasmid containing the full-length human *FOS* cDNA (NM\_005252.4) was purchased from Addgene (Plasmid #59140). The full-length *FOS* cDNA was cloned into the pCS2 vector and *FOS* mRNA was generated using the mMessage mMachine Sp6 kit (Ambion, Austin, TX). mRNA was resuspended in nuclease-free water to a stock concentration of 2 ng/ $\mu$ L and diluted to 0.5 ng/ $\mu$ L in 0.1 M KCl for injections. Fos F0 crispants were created using IDT Alt-R™ CRISPR-Cas9 System (Coralville, IA). Two Crispr RNAs (crRNAs) specific to Fos gene (*fos* crRNA1: CGA GCAAGGAAATACAAGAC and *fos* crRNA2: GGTTGGGGAATT CAAGGAGT) were hybridized separately with trans activating crispr RNA (tracrRNA) to form a functional gRNA complex. 60  $\mu$ M of each gRNA was incubated with 5  $\mu$ g/ $\mu$ L of Cas9 protein (Alt-R® S.p. Cas9 Nuclease, IDT) for 10 min at 37°C to generate the ribonucleoprotein (RNP) complex. Equimolar amounts of the two RNPs were mixed and injected into the zebrafish embryos. For all zebrafish injections, one-cell embryos were injected with 1 nL of MO, mRNA or RNPs.

## Zebrafish facial analytics based on coordinate extrapolate system (zFACE)

Embryos were fixed in 4% paraformaldehyde (PFA) (Sigma) in 1X phosphate buffered saline with Triton X-100 (PBST) at room temperature for 4 h and stained with 0.2 mg/L DAPI (Life Technologies) for 30 min at room temperature. Embryos were mounted rostrally in 1% low-melt agarose (Research Products International, Mount Prospect, IL) and imaged with Zeiss LSM 800 Confocal Microscope (Thornwood, NJ). Twenty-six anatomic landmarks including eyes, olfactory pits, neuromasts and mouth were identified from the confocal images and measurements between these landmarks were calculated to extract phenotypic features and understand which anatomical structures were altered as a result of *fos* knockdown. ANOVA and Tukey's test for multiple comparisons was applied on each measurement and Bonferroni correction for 39 measurements was applied to determine statistical significance. GraphPad Prism 9.0.0 was used to plot and visualize the data.

## Multivariate analysis of zFACE measurements and landmarks

Dimensionality reduction was performed using Principal Component Analysis (PCA) in StataIC 14 (StataCorp. 2015). Components with an eigenvalue of greater than or equal to 1 (following the Kaiser-Guttman method) were retained for analysis. Promax rotation, which accounts for correlations between the different factors (zFACE measurements) was used because a high correlation was observed/expected between features calculated using shared landmarks. Principal component (PC) scores were predicted and logistic regression models were utilized to regress morphant/crispant status by PC scores.

Additionally, to focus on facial shape and remove variation due to size, position, or rotation, the 2D landmark data points from the 26 zFACE coordinates were uploaded into MorphoJ version 1.07 A and principal axes Procrustes superimposition was performed (Klingenberg, 2011). After Procrustes transformation, PCA was used to examine general shape variation in the combined groups. Additionally, discriminant function analysis (DFA), which maximizes the between-group variance relative to within-group variance, was used to pinpoint shape in *fos* morphants/crispant compared to controls. Mean Procrustes distance with 10,000 permutations was used to statistically test shape differences between control and experimental groups.

## Skeletal staining

Alcian blue (Anatech LTD.) and alizarin red (Sigma-Aldrich) staining was performed using standard techniques (Kimmel and Trammell 1981) to visualize the bone and cartilage structures. Briefly, 5-8dpf embryos were collected and fixed in 2% PFA/1X PBST for 1 h at room temperature and stored in methanol overnight at  $-20^{\circ}\text{C}$ . After removing methanol, embryos were incubated in 0.04% alcian blue solution (100 mmol/L Tris, pH 7.5, 10 mmol/L  $\text{MgCl}_2$ , 64% ethanol) overnight at room temperature. They were destained in 3%  $\text{H}_2\text{O}_2$ /0.5% KOH for 10 min at room temperature and then stained in 0.02% alizarin red solution (100 mmol/L Tris, pH 7.5, 25% glycerol) for 30 min at room temperature. Embryos were then destained in 50% glycerol/0.1% KOH

for 30 min and stored in 50% glycerol. Imaging was performed using the LAS Montage Module (Leica). For visualizing teeth, a 0.5% Alizarin Red solution was used to stain fixed *sox10:gfp* reporter embryos for 1 h.

## Fluorescent signal and cell measurements

Periderm cells were measured in Zen software (Zeiss, Thornwood, NJ) using the contour graphics tool. Midface and perioral cells were analyzed separately due to already existing differences in their size. In each individual embryo, 10 cells were measured from each region and at least 10 individuals were analyzed from each group.

Average fluorescence signal was measured in ImageJ (Schneider et al., 2012). Wnt-responsive cells were counted using the Spots detection tool and automatic detection settings in Imaris software (Bitplane, Oxford Instruments) utilizing default settings with at least 3 animals analyzed for each condition.

## Caspase assay

Embryos were fixed at 1dpf in 2% PFA/1XPBS overnight at  $4^{\circ}\text{C}$ . After washing, they were incubated with block solution (1% DMSO, 2 mg/ml BSA, 0.5% Triton X-100, 10% inactivated goat serum in PBS) for 2 h at room temperature, washed and then incubated with 1:700 dilution of Rabbit Activated Caspase 3 (BD Biosciences, Franklin Lakes, NJ) in block solution overnight at  $4^{\circ}\text{C}$ . 1:150 dilution of Donkey Anti-Rabbit 647 (Molecular Probes, Eugene, OR) was used for secondary antibody staining. Washed embryos were mounted in 1% low-melt agarose for confocal imaging.

## HCR assay

HCR assay was performed using Molecular Instruments Multiplexed v3.0 protocol and reagents (Molecular Instruments, Los Angeles, CA). Briefly, embryos were fixed at different stages in 2% PFA/1XPBS overnight at  $4^{\circ}\text{C}$ . They were pre-hybridized with probe hybridization buffer for 30 min at  $37^{\circ}\text{C}$ , then incubated with 4 nM of the probe (*fosab* HCR probe set B2 Alexa Fluor 546) in probe hybridization buffer overnight at  $37^{\circ}\text{C}$ . Embryos were washed with 5X SSCT and incubated with amplification buffer for 30 min at room temperature. 30 pmol of hairpins h1 and h2 corresponding to the probe were snap cooled (heated at  $95^{\circ}\text{C}$  for 90 s and cooled to room temperature in a dark drawer), diluted in 500  $\mu\text{L}$  of amplification buffer and added to the embryos for overnight incubation in the dark at room temperature. Washed embryos were mounted in 1% low-melt agarose for confocal imaging.

## Quantitative PCR

Total RNA was extracted from a group of 5 embryos using Trizol (Invitrogen) as described previously (Chiquet et al., 2018). Further purification was done using RNeasy Mini Kit (Qiagen). The purified RNA was reverse transcribed to cDNA using Quantitect<sup>TM</sup> Reverse Transcription Kit (Qiagen). Gene expression of different *fos* family genes in zebrafish was analyzed using Quantitect<sup>TM</sup> Primer Assays (Qiagen) for

each individual gene—*fosaa*, *fosab*, *fosb*, *fosl1a*, *fosl1b* and *fosl2* – and data was normalized using beta-actin (*actb1*) as an endogenous control. All samples were run in triplicate and compared using Student's t-tests.

## Pharmacological treatments

AP-1 inhibitor SR 11302 (Tocris Bio-Techne, Minneapolis, MN; Catalog No.2476, Batch No.7, Minimum Purity>98%) was dissolved in DMSO to prepare a stock solution. Varying concentrations of drug (1, 5, and 10  $\mu$ M) were added to embryo dishes starting at either 1 or 2 dpf with daily media changes until collection at 5 dpf. The controls included treatment with the same volume of DMSO and untreated dishes.

## Summary statement

Perturbation of *fos*, a candidate gene associated with nonsyndromic cleft lip and palate in humans, causes a distinctive orofacial phenotype in zebrafish as a result of abnormal development of craniofacial tissues. Disruption of *fos* in the oral epithelial, cranial neural crest and Wnt responsive cell populations around the oral cavity causes anomalies that suggest a potential role in the etiology of NSCLP.

## Data availability statement

The original contributions presented in the study are included in the article/[Supplementary Material](#), further inquiries can be directed to the corresponding author.

## Ethics statement

The animal study was reviewed and approved by UTHealth Animal Welfare Committee.

## Author contributions

LM, BT, AL, GE and JH conceptualized the project and methodology. LM, BT, QY, FC and SM performed all the experiments and subsequent analyses. SH provided assistance with statistical analysis. LM and BT wrote the

manuscript and AL, GE and JH edited the manuscript. All authors contributed to the article and approved the submitted version.

## Funding

This study was supported by NIH grants R01-DE11931 (to JH) and F31-DE28187 (to LM); the Gulf Coast Consortium Collaborative Research Award to JH and GE; and the Cancer Prevention Research Institute of Texas, RR140077; the National Institute of General Medical Sciences, National Institutes of Health, R01GM124043; and the Mark and Linda Quick Basic Science Award to GE.

## Acknowledgments

We thank Christian Urbina for morphometric data analysis assistance.

## Conflict of interest

The authors declare that the research was conducted in the absence of any commercial or financial relationships that could be construed as a potential conflict of interest.

## Publisher's note

All claims expressed in this article are solely those of the authors and do not necessarily represent those of their affiliated organizations, or those of the publisher, the editors and the reviewers. Any product that may be evaluated in this article, or claim that may be made by its manufacturer, is not guaranteed or endorsed by the publisher.

## Supplementary material

The Supplementary Material for this article can be found online at: <https://www.frontiersin.org/articles/10.3389/fcell.2023.1141893/full#supplementary-material>

## References

- Alfaqeeh, S., Oralova, V., Foxworthy, M., Matalova, E., Grigoriadis, A. E., and Tucker, A. S. (2015). Root and eruption defects in c-fos mice are driven by loss of osteoclasts. *J. Dent. Res.* 94 (12), 1724–1731. doi:10.1177/0022034515608828
- Boer, E. F., Jette, C. A., and Stewart, R. A. (2016). Neural crest migration and survival are susceptible to morpholino-induced artifacts. *PLoS One* 11 (12), e0167278. doi:10.1371/journal.pone.0167278
- Brugmann, S. A., Goodnough, L. H., Gregorieff, A., Leucht, P., ten Berge, D., Fuerer, C., et al. (2007). Wnt signaling mediates regional specification in the vertebrate face. *Development* 134 (18), 3283–3295. doi:10.1242/dev.005132
- Buglo, E., Sarmiento, E., Martuscelli, N. B., Sant, D. W., Danzi, M. C., Abrams, A. J., et al. (2020). Genetic compensation in a stable *slc25a46* mutant zebrafish: A case for using F0 crispr mutagenesis to study phenotypes caused by inherited disease. *PLoS One* 15 (3), e0230566. doi:10.1371/journal.pone.0230566
- Burger, A., Lindsay, H., Felker, A., Hess, C., Anders, C., Chiavacci, E., et al. (2016). Maximizing mutagenesis with solubilized CRISPR-Cas9 ribonucleoprotein complexes. *Development* 143 (11), 2025–2037. doi:10.1242/dev.134809
- Carney, T. J., Dutton, K. A., Greenhill, E., Delfino-Machin, M., Dufourcq, P., Blader, P., et al. (2006). A direct role for Sox10 in specification of neural crest-derived sensory neurons. *Development* 133 (23), 4619–4630. doi:10.1242/dev.02668
- Chai, Y., and Maxson, R. E., Jr. (2006). Recent advances in craniofacial morphogenesis. *Dev. Dyn.* 235 (9), 2353–2375. doi:10.1002/dvdy.20833
- Chen, J., Lan, Y., Baek, J. A., Gao, Y., and Jiang, R. (2009). Wnt/beta-catenin signaling plays an essential role in activation of odontogenic mesenchyme during early tooth development. *Dev. Biol.* 334 (1), 174–185. doi:10.1016/j.ydbio.2009.07.015

- Chen, J., Zhang, E., Zhang, W., Liu, Z., Lu, P., Zhu, T., et al. (2017). Fos promotes early stage teno-lineage differentiation of tendon stem/progenitor cells in tendon. *Stem Cells Transl. Med.* 6 (11), 2009–2019. doi:10.1002/sctm.15-0146
- Chiquet, B. T., Lidral, A. C., Stal, S., Mulliken, J. B., Moreno, L. M., Arcos-Burgos, M., et al. (2007). CRISPLD2: A novel NSCLP candidate gene. *Hum. Mol. Genet.* 16 (18), 2241–2248. doi:10.1093/hmg/ddm176
- Chiquet, B. T., Yuan, Q., Swindell, E. C., Maili, L., Plant, R., Dyke, J., et al. (2018). Knockdown of Crisppld2 in zebrafish identifies a novel network for nonsyndromic cleft lip with or without cleft palate candidate genes. *Eur. J. Hum. Genet.* 26 (10), 1441–1450. doi:10.1038/s41431-018-0192-5
- Choi, H. M. T., Schwarzkopf, M., Fornace, M. E., Acharya, A., Artavanis, G., Stegmaier, J., et al. (2018). Third-generation *in situ* hybridization chain reaction: multiplexed, quantitative, sensitive, versatile, robust. *Development* 145 (12), dev165753. doi:10.1242/dev.165753
- Cordero, D. R., Brugmann, S., Chu, Y., Bajpai, R., Jame, M., and Helms, J. A. (2011). Cranial neural crest cells on the move: their roles in craniofacial development. *Am. J. Med. Genet. A* 155A (2), 270–279. doi:10.1002/ajmg.a.33702
- Cusack, B. J., Parsons, T. E., Weinberg, S. M., Vieira, A. R., and Szabo-Rogers, H. L. (2017). Growth factor signaling alters the morphology of the zebrafish ethmoid plate. *J. Anat.* 230 (5), 701–709. doi:10.1111/joa.12592
- Dash, S., and Trainor, P. A. (2020). The development, patterning and evolution of neural crest cell differentiation into cartilage and bone. *Bone* 137, 115409. doi:10.1016/j.bone.2020.115409
- Dixon, M. J., Marazita, M. L., Beaty, T. H., and Murray, J. C. (2011). Cleft lip and palate: understanding genetic and environmental influences. *Nat. Rev. Genet.* 12 (3), 167–178. doi:10.1038/nrg2933
- Dougherty, M., Kamel, G., Grimaldi, M., Gfrerer, L., Shubinets, V., Ethier, R., et al. (2013). Distinct requirements for *wnt9a* and *irf6* in extension and integration mechanisms during zebrafish palate morphogenesis. *Development* 140 (1), 76–81. doi:10.1242/dev.080473
- Duncan, K. M., Mukherjee, K., Cornell, R. A., and Liao, E. C. (2017). Zebrafish models of orofacial clefts. *Dev. Dyn.* 246 (11), 897–914. doi:10.1002/dvdy.24566
- Durchdewald, M., Angel, P., and Hess, J. (2009). The transcription factor *fos*: A janus-type regulator in health and disease. *Histol. Histopathol.* 24 (11), 1451–1461. doi:10.14670/HH-24.1451
- Eames, B. F., DeLaurier, A., Ullmann, B., Huyck, T. R., Nichols, J. T., Dowd, J., et al. (2013). FishFace: interactive atlas of zebrafish craniofacial development at cellular resolution. *BMC Dev. Biol.* 13, 23. doi:10.1186/1471-213X-13-23
- Eberhart, J. K., He, X., Swartz, M. E., Yan, Y. L., Song, H., Boling, T. C., et al. (2008). MicroRNA *Mir140* modulates *Pdgf* signaling during palatogenesis. *Nat. Genet.* 40 (3), 290–298. doi:10.1038/ng.82
- El Sergani, A. M., Brandebura, S., Padilla, C., Butali, A., Adeyemo, W. L., Valencia-Ramirez, C., et al. (2020). Parents of children with nonsyndromic orofacial clefting show altered palate shape. *Cleft Palate Craniofac J.* 1055665620967235, 847–853. doi:10.1177/1055665620967235
- Fraser, F. C., and Pashayan, H. (1970). Relation of face shape to susceptibility to congenital cleft lip. A preliminary report. *J. Med. Genet.* 7 (2), 112–117. doi:10.1136/jmg.7.2.112
- Ge, X., Shi, Q. M., Ding, Z., Ju, Q., Wang, H., Wang, Q., et al. (2018). Association between CRISPLD2 polymorphisms and the risk of nonsyndromic clefts of the lip and/or palate: A meta-analysis. *Cleft Palate Craniofac J.* 55 (3), 328–334. doi:10.1177/1055665617738995
- Gong, Z., Ju, B., Wang, X., He, J., Wan, H., Sudha, P. M., et al. (2002). Green fluorescent protein expression in germ-line transmitted transgenic zebrafish under a stratified epithelial promoter from keratin8. *Dev. Dyn.* 223 (2), 204–215. doi:10.1002/dvdy.10051
- Gorlin, R. J., Cohen, M. M., and Hennekam, R. C. M. (2011). *Syndromes of the head and neck*. Fourth Edition ed. New York: Oxford University Press.
- Green, R. M., Feng, W., Phang, T., Fish, J. L., Li, H., Spritz, R. A., et al. (2015). *Tfap2a*-dependent changes in mouse facial morphology result in clefting that can be ameliorated by a reduction in *Fgf8* gene dosage. *Dis. Model Mech.* 8 (1), 31–43. doi:10.1242/dmm.017616
- Grigoriadis, A. E., Wang, Z. Q., and Wagner, E. F. (1995). Fos and bone cell development: lessons from a nuclear oncogene. *Trends Genet.* 11 (11), 436–441. doi:10.1016/s0168-9525(00)89142-8
- Hammond, N. L., Dixon, J., and Dixon, M. J. (2019). Periderm: life-cycle and function during orofacial and epidermal development. *Semin. Cell Dev. Biol.* 91, 75–83. doi:10.1016/j.semcdb.2017.08.021
- He, F., and Chen, Y. (2012). Wnt signaling in lip and palate development. *Front. Oral Biol.* 16, 81–90. doi:10.1159/000337619
- Ji, Y., Garland, M. A., Sun, B., Zhang, S., Reynolds, K., McMahon, M., et al. (2020). Cellular and developmental basis of orofacial clefts. *Birth Defects Res.* 112 (19), 1558–1587. doi:10.1002/bdr2.1768
- Jiang, R., Bush, J. O., and Lidral, A. C. (2006). Development of the upper lip: morphogenetic and molecular mechanisms. *Dev. Dyn.* 235 (5), 1152–1166. doi:10.1002/dvdy.20646
- Johnson, R. S., Spiegelman, B. M., and Papaioannou, V. (1992). Pleiotropic effects of a null mutation in the *c-fos* proto-oncogene. *Cell* 71 (4), 577–586. doi:10.1016/0092-8674(92)90592-z
- Jussila, M., and Thesleff, I. (2012). Signaling networks regulating tooth organogenesis and regeneration, and the specification of dental mesenchymal and epithelial cell lineages. *Cold Spring Harb. Perspect. Biol.* 4 (4), a008425. doi:10.1101/cshperspect.a008425
- Klingenberg, C. P. (2011). MorphoJ: an integrated software package for geometric morphometrics. *Mol. Ecol. Resour.* 11 (2), 353–357. doi:10.1111/j.1755-0998.2010.02924.x
- Letra, A., Menezes, R., Cooper, M., Fonseca, R., Tropp, S., Govil, M., et al. (2010). Crisppld2 variants including a C471T silent mutation may contribute to nonsyndromic cleft lip with or without cleft palate. *Cleft Palate Craniofac J.* 48, 363–370. doi:10.1597/09-227
- Maili, L., Ruiz, O. E., Kahan, P. H., Chiu, F., Larson, S. T., Hashmi, S., et al. (2023). Facial analytics based on a coordinate extrapolation system (zFACE) for morphometric phenotyping of developing zebrafish. *Dis Model Mech* 16 (6), dmm049868. doi:10.1242/dmm.049868
- Marazita, M. L., and Mooney, M. P. (2004). Current concepts in the embryology and genetics of cleft lip and cleft palate. *Clin. Plast. Surg.* 31 (2), 125–140. doi:10.1016/S0094-1298(03)00138-X
- Martinez Arias, A., and Steventon, B. (2018). On the nature and function of organizers. *Development* 145 (5), dev159525. doi:10.1242/dev.159525
- McLennan, R., McKinney, M. C., Teddy, J. M., Morrison, J. A., Kasemeier-Kulesa, J. C., Ridenour, D. A., et al. (2020). Neural crest cells bulldoze through the microenvironment using Aquaporin 1 to stabilize filopodia. *Development* 147 (1), dev185231. doi:10.1242/dev.185231
- Mijiti, A., Ling, W., Maimaiti, A., Tuerdi, M., Tuerxun, J., and Moming, A. (2015). Preliminary evidence of an interaction between the CRISPLD2 gene and nonsyndromic cleft lip with or without cleft palate (nsCL/P) in Xinjiang Uyghur population, China. *Int. J. Pediatr. Otorhinolaryngol.* 79 (2), 94–100. doi:10.1016/j.ijporl.2014.10.043
- Milde-Langosch, K. (2005). The Fos family of transcription factors and their role in tumorigenesis. *Eur. J. Cancer* 41, 2449–2461. doi:10.1016/j.ejca.2005.08.008
- Mork, L., and Crump, G. (2015). Zebrafish craniofacial development: A window into early patterning. *Curr. Top. Dev. Biol.* 115, 235–269. doi:10.1016/bs.ctdb.2015.07.001
- Moro, E., Ozhan-Kizil, G., Mongera, A., Beis, D., Wierzbicki, C., Young, R. M., et al. (2012). *In vivo* Wnt signaling tracing through a transgenic biosensor fish reveals novel activity domains. *Dev. Biol.* 366 (2), 327–340. doi:10.1016/j.ydbio.2012.03.023
- Murillo-Rincon, A. P., and Kaucka, M. (2020). Insights into the complexity of craniofacial development from a cellular perspective. *Front. Cell Dev. Biol.* 8, 620735. doi:10.3389/fcell.2020.620735
- Parsons, T. E., Kristensen, E., Hornung, L., Diewert, V. M., Boyd, S. K., German, R. Z., et al. (2008). Phenotypic variability and craniofacial dysmorphology: increased shape variance in a mouse model for cleft lip. *J. Anat.* 212 (2), 135–143. doi:10.1111/j.1469-7580.2007.00845.x
- Perrimon, N., Pitsouli, C., and Shilo, B. Z. (2012). Signaling mechanisms controlling cell fate and embryonic patterning. *Cold Spring Harb. Perspect. Biol.* 4 (8), a005975. doi:10.1101/cshperspect.a005975
- Raterman, S. T., Metz, J. R., Wagener, F., and Von den Hoff, J. W. (2020). Zebrafish models of craniofacial malformations: interactions of environmental factors. *Front. Cell Dev. Biol.* 8, 600926. doi:10.3389/fcell.2020.600926
- Reynolds, K., Kumari, P., Sepulveda Rincon, L., Gu, R., Ji, Y., Kumar, S., et al. (2019). Wnt signaling in orofacial clefts: crosstalk, pathogenesis and models. *Dis. Model Mech.* 12 (2), dmm037051. doi:10.1242/dmm.037051
- Ribatti, D., and Santoiemma, M. (2014). Epithelial-mesenchymal interactions: A fundamental developmental Biology mechanism. *Int. J. Dev. Biol.* 58 (5), 303–306. doi:10.1387/ijdb.140143dr
- Richardson, R. J., Hammond, N. L., Coulombe, P. A., Saloranta, C., Nousiainen, H. O., Salonen, R., et al. (2014). Periderm prevents pathological epithelial adhesions during embryogenesis. *J. Clin. Invest.* 124 (9), 3891–3900. doi:10.1172/JCI171946
- Rodriguez-Berdini, L., Ferrero, G. O., Bustos Plonka, F., Cardozo Gizzi, A. M., Prucca, C. G., Quiroga, S., et al. (2020). The moonlighting protein c-Fos activates lipid synthesis in neurons, an activity that is critical for cellular differentiation and cortical development. *J. Biol. Chem.* 295 (26), 8808–8818. doi:10.1074/jbc.RA119.010129
- Rossi, A., Kontarakis, Z., Gerri, C., Nolte, H., Holper, S., Kruger, M., et al. (2015). Genetic compensation induced by deleterious mutations but not gene knockdowns. *Nature* 524 (7564), 230–233. doi:10.1038/nature14580
- Schilling, T. F., and Le Pabic, P. (2009). Fishing for the signals that pattern the face. *J. Biol.* 8 (11), 101. doi:10.1186/jbiol205
- Schneider, C. A., Rasband, W. S., and Eliceiri, K. W. (2012). NIH image to ImageJ: 25 years of image analysis. *Nat. Methods* 9 (7), 671–675. doi:10.1038/nmeth.2089

- Shen, X., Liu, R. M., Yang, L., Wu, H., Li, P. Q., Liang, Y. L., et al. (2011). The CRISPLD2 gene is involved in cleft lip and/or cleft palate in a Chinese population. *Birth defects Res. Part A, Clin. Mol. Teratol.* 91 (10), 918–924. doi:10.1002/bdra.20840
- Sherwood, D. R., Butler, J. A., Kramer, J. M., and Sternberg, P. W. (2005). FOS-1 promotes basement-membrane removal during anchor-cell invasion in *C. elegans*. *Cell* 121 (6), 951–962. doi:10.1016/j.cell.2005.03.031
- Smeyne, R. J., Schilling, K., Oberdick, J., Robertson, L., Luk, D., Curran, T., et al. (1993a). A fos-lac Z transgenic mouse that can be used for neuroanatomic mapping. *Adv. Neurol.* 59, 285–291. Retrieved from <http://www.ncbi.nlm.nih.gov/pubmed/8420113>.
- Smeyne, R. J., Vendrell, M., Hayward, M., Baker, S. J., Miao, G. G., Schilling, K., et al. (1993b). Continuous c-fos expression precedes programmed cell death *in vivo*. *Nature* 363 (6425), 166–169. doi:10.1038/363166a0
- Soukup, V., Horacek, I., and Cerny, R. (2013). Development and evolution of the vertebrate primary mouth. *J. Anat.* 222 (1), 79–99. doi:10.1111/j.1469-7580.2012.01540.x
- Swartz, M. E., Sheehan-Rooney, K., Dixon, M. J., and Eberhart, J. K. (2011). Examination of a palatogenic gene program in zebrafish. *Dev. Dyn.* 240 (9), 2204–2220. doi:10.1002/dvdy.22713
- Swindell, E. C., Yuan, Q., Maili, L. E., Tandon, B., Wagner, D. S., and Hecht, J. T. (2015). Crisppld2 is required for neural crest cell migration and cell viability during zebrafish craniofacial development. *Genesis* 53 (10), 660–667. doi:10.1002/dvg.22897
- Van der Heyden, C., and Huyseune, A. (2000). Dynamics of tooth formation and replacement in the zebrafish (*Danio rerio*) (Teleostei, Cyprinidae). *Dev. Dyn.* 219 (4), 486–496. doi:10.1002/1097-0177(2000)9999:9999::AID-DVDY1069>3.0.CO;2-Z
- Velazquez, F. N., Prucca, C. G., Etienne, O., D'Astolfo, D. S., Silvestre, D. C., Boussin, F. D., et al. (2015). Brain development is impaired in c-fos  $-/-$  mice. *Oncotarget* 6 (19), 16883–16901. doi:10.18632/oncotarget.4527
- Wagner, E. F. (2002). Functions of AP1 (Fos/Jun) in bone development. *Ann. Rheum. Dis.* 61, ii40–42. doi:10.1136/ard.61.suppl\_2.ii40
- Wang, Q., Liu, H., Wang, Q., Zhou, F., Liu, Y., Zhang, Y., et al. (2017). Involvement of c-Fos in cell proliferation, migration, and invasion in osteosarcoma cells accompanied by altered expression of Wnt2 and Fzd9. *PLoS One* 12 (6), e0180558. doi:10.1371/journal.pone.0180558
- Weinberg, S. M., Maher, B. S., and Marazita, M. L. (2006a). Parental craniofacial morphology in cleft lip with or without cleft palate as determined by cephalometry: A meta-analysis. *Orthod. Craniofac. Res.* 9 (1), 18–30. doi:10.1111/j.1601-6343.2006.00339.x
- Weinberg, S. M., Naidoo, S. D., Bardi, K. M., Brandon, C. A., Neiswanger, K., Resick, J. M., et al. (2009). Face shape of unaffected parents with cleft affected offspring: combining three-dimensional surface imaging and geometric morphometrics. *Orthod. Craniofac. Res.* 12 (4), 271–281. doi:10.1111/j.1601-6343.2009.01462.x
- Weinberg, S. M., Neiswanger, K., Martin, R. A., Mooney, M. P., Kane, A. A., Wenger, S. L., et al. (2006b). The pittsburgh oral-facial cleft study: expanding the cleft phenotype. Background and justification. *Cleft Palate Craniofac. J.* 43 (1), 7–20. doi:10.1597/04-122r1.1
- Weinberg, S. M., Neiswanger, K., Richtsmeier, J. T., Maher, B. S., Mooney, M. P., Siegel, M. I., et al. (2008). Three-dimensional morphometric analysis of craniofacial shape in the unaffected relatives of individuals with nonsyndromic orofacial clefts: A possible marker for genetic susceptibility. *Am. J. Med. Genet. A* 146A (4), 409–420. doi:10.1002/ajmg.a.32177
- M. Westerfield (Editor) (1993). *The zebrafish book: A guide for the laboratory use of zebrafish (brachydanio rerio)* (Eugene, OR: M. Westerfield).
- Yano, H., Ohtsuru, A., Ito, M., Fujii, T., and Yamashita, S. (1996). Involvement of c-Fos proto-oncogene during palatal fusion and interdigital space formation in the rat. *Dev. Growth Differ.* 38 (4), 351–357. doi:10.1046/j.1440-169X.1996.t01-3-00003.x
- Yelick, P. C., and Schilling, T. F. (2002). Molecular dissection of craniofacial development using zebrafish. *Crit. Rev. Oral Biol. Med.* 13 (4), 308–322. doi:10.1177/154411130201300402
- Young, N. M., Wat, S., Diewert, V. M., Browder, L. W., and Hallgrímsson, B. (2007). Comparative morphometrics of embryonic facial morphogenesis: implications for cleft-lip etiology. *Anat. Rec. Hob. N.J.* 290 (1), 123–139. doi:10.1002/ar.20415
- Yuan, Q., Chiquet, B. T., Devault, L., Warman, M. L., Nakamura, Y., Swindell, E. C., et al. (2012). Craniofacial abnormalities result from knock down of nonsyndromic clefting gene, *crisppld2*, in zebrafish. *Genesis* 50 (12), 871–881. doi:10.1002/dvg.22051